

Prediction of the cutting tool wear during dry hard turning of AISI D2 steel by using models based on Learning process and GA polyfit

Article Info:

Article history: Received 2023-10-10/ Accepted 2023-12-10 / Available online 2023-12-28

doi: 10.18540/jcecv19iss12pp18297



Khaled Djellouli

ORCID: <https://orcid.org/0000-0003-1052-4951>

Research Laboratory of Industrial Technologies, Faculty of Applied Sciences, University of Tiaret,
B. P. 78 Zaâroua 14000 Tiaret, Algeria
E-mail: djelloulikhld@gmail.com

Kamel Haddouche

ORCID: <https://orcid.org/0000-0002-7084-0246>

Research Laboratory of Industrial Technologies, Faculty of Applied Sciences, University of Tiaret,
B. P. 78 Zaâroua 14000 Tiaret, Algeria
E-mail: haddouchekam@gmail.com

Mostefa Belarbi

ORCID: <https://orcid.org/0000-0002-6722-5912>

LIM Research laboratory, University of Tiaret, B. P. 78 Zaâroua 14000 Tiaret, Algeria
E-mail: belarbimostefa@yahoo.fr

Zoubir Aich

ORCID: <https://orcid.org/0000-0002-1325-9121>

Research Laboratory of Industrial Technologies, Faculty of Applied Sciences, University of Tiaret,
B. P. 78 Zaâroua 14000 Tiaret, Algeria
E-mail: aichzoubir7@gmail.com

Abstract

In this paper, we are interested in the prediction of flank wear through dry hard turning of AISI D2 steel with a mixed alumina insert. In the machining process, the cutting tool is principally affected by two kinds of wear: flank and crater wear. The latter are criteria for cessation of the tool function. In the absence of a real-time wear sensor, it is necessary to know or track wear with the view to prevent tool damage. For this purpose, the current research focuses on the development of predictive models of flank wear based on Artificial Neural Network (ANN), Gaussian Process Regression (GPR), Support Vector Machine (SVM), and Polynomial Fit using Genetic Algorithm (GAPOLYFITN). The simulation process involves considering input variables including feed (f), cutting speed (V_c), and cutting time (t_c); the output is the flank wear (VB). To assess the statistical efficacy of the predictive models, some performance indicators were employed, including the R-squared statistic- R^2 , Mean Square Error-MSE, Mean Absolute Error-MAE, and Mean Absolute Percentage Error-MAPE. The results, for the present case study, show that the R-squared statistic ranges from 0.85 to 0.99, the MSE is between 0.000046 and 0.000177, the MAE ranges from 0.002958 to 0.009336, and the value of MAPE varies from 3.50 to 9.60%. The predictive capability of GPR and GAPOLYFITN in determining flank wear are the best, as they exhibit high (R^2), and lower values of MSE, MAE, and MAPE. The powerful predictive model of flank wear is the GPR because it provides $R^2 = 0.96$, $MSE = 4.6e-5$, $MAE = 0.002958$, and $MAPE = 3.50\%$.

Keywords: Flank wear. Ceramic insert. AISI D2 steel. Hard turning. Learning process. GA.

1. Introduction

The modeling of the tool's wear is a significant challenge of the cutting theory because it is quite difficult to construct a theoretical model that effectively describes the wear mechanisms (mechanical, thermal, and metallurgical). In machining, the cutting tool's wear can be characterized as a detrimental process that affects the machined surface, resulting in gradual alterations to the tool's geometry, state of contact surfaces, and tool properties. Generally, these alterations decrease the cutting tool capacity. In addition, the wear can directly influence various factors of the machining process, including cutting force, temperature, product quality, etc. It is rational to assert that the initial factor influencing tool longevity is wear, which may be categorized into abrasion, adhesion, erosion, fretting, and chemical wear. The tool's life is contingent upon the magnitude of its wear; as a result, the time and cost of machining are related to the wear. For this, the manufacturers of tools continually enhance the cutting-edge, coating, geometry, and overall material of the tool. Finally, the tool wear must be controlled and correctly predicted to ensure better performance of the cutting process. In this context, several studies have been conducted by numerous researchers to address the task of modeling or predicting the wear of the cutting tool but we will cite some related to the wear during the turning of hard steel (AISI D2).

Özel *et al.* (2007) developed MLR and ANN models for predicting surface roughness and tool flank wear in the finish-turning of hard steel (AISI D2) with wiper ceramic insert. Their results demonstrate that neural network models are adept at prediction across various cutting conditions. Quiza *et al.* (2008) compared statistical models in ANN on predicting tool wear. For the statistical models, experimental data were used to adjust three regressions, namely linear, quadratic, and potential. For their study, the neural network model has demonstrated superior ability in predicting tool wear. Davim *et al.* (2007) in their study, considers the impact of wiper inserts in contrast to conventional inserts on machinability parameters such as (cutting forces, surface roughness, and tool wear). Using wiper ceramic inserts enabled the attainment of machined surfaces with a roughness average (Ra) of less than 0.8 μm . As a result, it is feasible to achieve surface qualities in a workpiece of mechanical precision within ($IT < 7$). The paper of Khan *et al.* (2017) reports on tool wear/life, material removal, and workpiece surface roughness when utilizing mixed alumina tool inserts with three different nose radii. Their results demonstrate that flank wear leads to catastrophic tool failure at the combination of the highest nose radius and feed rate. After, their investigation, the study revealed that cutting speed exerts a notable impact on tool wear/life, contributing 55.38% followed by feed rate (13.72%) and depth of cut (11.43%).

The PCBN, among the likes of carbide and ceramic cutters, is widely accepted for machining AISI D2 and serves as a cost-effective substitute for costly grinding operations. Arsecularathe *et al.* (2006) performed an empirical investigation into the machining of AISI D2 steel utilizing PCBN tools. Their results indicate that, under the specified conditions, the correlation between tool longevity and cutting parameters can be described through a Taylor-type tool life equation. Muhammad *et al.* (2018) attempted to explore the effect of wipers and conventional insets during the turning of AISI D2 steel with PCBN tools. In this research inserts (wiper and conventional) having three different tools of nose radius were evaluated. The research revealed that in profile turning, conventional inserts with a larger nose radius outperformed the other two inserts in surface roughness and dimensional accuracy. In the case of wiper inserts, the surface roughness and dimensional accuracy outcomes did not surpass those of conventional inserts. Choudhury *et al.* (2023) investigated the impact of the surface texturing of a coated carbide tool on the flank face while machining AISI D2 steel, and then the artificial neural network was implemented for the prediction of the surface finish and flank wear. Contours are generated for surface roughness and flank wear for each texture using data generated from ANN. It was observed that the latter serves as a powerful predictive tool for the prediction of surface roughness of the machined surface and flank wear of the cutting tool. Tang *et al.* (2019) examined the wear characteristics of the PCBN tool during dry hard turning of AISI D2 at different hardness values under fixed cutting parameters. The results show that workpiece hardness has a significant effect on flank wear. Junaid *et al.* (2018)

analyzed a series of machinability studies focusing on tool wear and surface roughness in the finishing hard turning of AISI D2 steel utilizing PCBN, mixed ceramic, and coated carbide inserts. The findings indicate that tool wear was primarily influenced by cutting time and, to a lesser extent, by the hardness of the cutting tool. The relation between input variables and the response is ascertained through the utilization of a quadratic regression model.

For our contribution, we will develop predictive models to estimate the flank wear of the cutting tool based, on the one hand, on a learning process (ANN, GPR, SVM), and, on the other hand, on polynomial fit (GAPOLYFITN). For each predictive model, factors such as feed (f), cutting speed (V_c), and cutting time (t_c) are the input variables of the process; the output or response variable is the flank wear (VB). To assess the statistical efficacy of the predictive models, some performance indicators were employed, including the R-squared statistic- R^2 , Mean Square Error-MSE, Mean Absolute Error-MAE, and Mean Absolute Percentage Error-MAPE.

2. Modeling

2.1. ANN Approach

The ANN applied in this study utilizes a multilayer feed-forward structure, comprising input, hidden, and output layers. The ANN architecture includes an input layer for receiving inputs, an output layer that transmits final data to users, and a hidden layer that functions as an intermediary and remains isolated from direct interaction with the external environment. The hidden layer of the network is composed of interconnected neurons, serving as simple processing units. The output of a neuron (s_j) is done by Equation 1 (Hagan *et al.*, 2014).

$$s_j = g \left(\sum_{i=1}^m w_{ij} \cdot e_i - b_j \right) \quad (1)$$

When the activation level surpasses or equals the bias (b_j), the argument of the transfer function (g) applied to the sum of inputs attains a positive value (+1), while it remains zero otherwise. The bias is analogous to a weight applied to a fixed input of (-1). The weights (w_{ij}) assigned to neuron inputs (e_i) and the bias (b_j) are adjustable parameters.

To design the network the data are, generally, divided into two distinct databases: training and testing. A training algorithm is then employed to modify the coefficients (w_{ij}) and (b_j) to accomplish the preferred input-output relationship. Typically, the users have the flexibility to choose the transfer function, the number of hidden layers and neurons, and the training algorithm for giving good performances.

2.2. GPR model

The Gaussian processes model is a probabilistic supervised machine-learning framework that has been widely used for regression and classification tasks. GPR models are extensively utilized in machine learning applications due to their flexible representations and intrinsic capability to measure uncertainty in predictions. GPRs are extremely versatile regarding their application and can interpolate very well with small amounts of data available; however, they work best for low-dimensional problems, steady design spaces, and moderately sized datasets (Nikolaus *et al.*, 2021; Isabona *et al.*, 2023; Kong *et al.*, 2018).

Given a throughput dataset (x_i, y_i) for training with (x_i) and (y_i) defining the input and target variable quantities. The model function that connects (x_i) and (y_i) can be expressed by Equation 2 (Isabona *et al.*, 2023; Schulz *et al.*, 2018).

$$y_i = f(x_i) + \zeta_i \quad (2)$$

Where $\zeta_i = N(0, \sigma_i^2)$ indicates the mean noise model with (σ_i^2) being the variance.

Notice that for a distributed Gaussian Process, the observed target can be equally defined using Equation 3:

$$(x_i) \approx GP(m(x_i), K(X, X')) \quad (3)$$

With $K(X, X')$ articulating the covariance matrix and $m(x_i) = E[f(x_i)]$ being an expectation function for input (x_i) .

2.3. SVM model

A Support Vector Machine is a type of supervised learning algorithm used in machine learning to solve classification and regression tasks. The objective of the SVM algorithm is to find a hyperplane and to maximize the margin, which refers to the space between the hyperplane and the nearest data points (Salcedo-Sanz *et al.*, 2014; Gholami *et al.*, 2017). SVM models have been used for predicting the wear and life of cutting tools (Alajmi *et al.*, 2021; Kong *et al.*, 2017; Bagga *et al.*, 2023; Yu *et al.*, 2022). Similar to the ANN approach, the data are previously divided into training and test tables. After training, predictions will be generated for the test table as well as for the full data set. Finally, the coefficients of the SVM regression model will be extracted, including the support vectors, the coefficients, and the bias, which will be used to construct the equation of the predicted regression function, according to Equation 4:

$$f(x) = \sum_{i=1}^n \alpha_i K(X_i, x) + b \quad (4)$$

Where (α_i) are the coefficients obtained, (K) is the kernel function, (X_i) is the support vector, and (b) is the bias term.

2.4. Polynomial Fit Using Genetic Algorithm

In this case, the predictive model is performed by using the function GAPOLYFITN in Matlab software. This function incorporates the utilization of a genetic algorithm to optimize the structure of a polynomial fit that accurately represents experimental data (Clegg *et al.*, 2005); the aim is to decrease the number of terms needed for the polynomial fit, in comparison to least squares fit that using all possible terms. In addition, for this approach, a population of polynomial forms is generated, with each form representing a subset of the set of possible terms. The fitness of these forms is assessed based on their ability to fit the model data, as determined by the R-squared value obtained from the POLYFITN function. Through the application of a Genetic Algorithm, the population undergoes evolution based on their respective scores.

A polynomial with (n) variables can be represented in Equation 5:

$$a_1 \cdot x_1^2 \cdot x_2^4 \cdot x_3^1 \cdot x_n^p + a_2 \cdot x_1^6 \cdot x_2^3 \cdot x_3^1 \cdot x_n^p + \dots \quad (5)$$

Notice that the “term” refers to a group of variables such as. The number of terms within a polynomial can be determined by the following calculation: (m) denotes the maximum power utilized and (n) represents the number of variables.

3. Experimental data

Experimental data are obtained during the hard turning of a high carbon-chromium cold work tool steel (AISI D2) alloyed with molybdenum and vanadium (Özel *et al.*, 2007). Table 1 gives the typical chemical composition of the work material.

Table 1 – Chemical composition of AISI D2 steel (Özel *et al.*, 2007).

Element	C (%)	Si (%)	Mn (%)	Cr (%)	Mo (%)	V (%)
AISI D2	1.55	0.30	0.40	11.80	0.80	0.80
60 ± 1 HRC						

Notice that hard cutting offers an economical way of finishing machined surfaces as an alternative process to grinding. The capacity to create complicated shapes, good surface roughness, increased material removal rate, shorter finishing times, cost savings, and mitigating environmental problems are the main benefits of hard machining.

In addition, cold work tool steel is utilized in a wide variety of tools, dies, and other applications requiring great wear resistance. In addition, Furthermore, they have garnered significant interest because of their crucial use in industrial domains like blanking and forming dies, gauges, and collets. AISI D2 steels are used as dies, including trimming, coining, forming, thermosetting resin forming, punches, shear blades, thread rolls, press tools, pneumatic tools, etc. (Bourithis *et al.*, 2006; Abdul Rahim *et al.*, 2018).

In this study, the tool steel AISI D2 is the workpiece machined by a mixed alumina insert with wiper geometry (ISO code-CNGA 120408 S01525 WH) and coated by TiN Ref. GC6050; the used tool holder is DCLNL2020K12 (ISO). Table 2 summarizes the Design of Experiments (DOE).

Table 2 – Levels and values of explanatory factors.

Factors	V_c (m/min)	f (mm/rev)	t_c (min)
Levels	3	3	3
Values	80; 115; 150	0.05; 0.1; 0.15	5; 10; 15

The full factorial design with all possible combinations provides 27 couples of input-target data. Notice that the depth of cut is taken equal to 0.2 mm. Experimental data are reported in Tables 3 and 4.

The experimental dataset was split into two distinct databases for this study: the training and testing database. Out of the total 27 samples available, 70% of the samples were allocated for training, while the remaining 30% were reserved for testing. As outlined in Table 3, a total of 18 couples of input-target data were utilized for the models based on learning process. Notice that the user can build other training and test databases. In addition, these tables can be designed randomly but the prediction cannot be set in stone.

Figure 1 gives the histogram of experimental data of the flank wear (VB). The maximum value of the flank wear ($VB_{max} = 0.164$ mm) is obtained for the test n° 6 which has the input factors: $V_c = 80$ m/min, $f = 0.1$ mm/rev, and $t_c = 15$ min. The minimum value $VB_{min} = 0.047$ corresponds to the test n° 1 ($V_c = 80$ m/min, $f = 0.05$ mm/rev and $t_c = 5$ min). The mean value and the standard deviation are equal respectively to 0.10422 and 0.03198.

Table 3 – Training dataset.

Test n°	Input variables			Measured flank wear
	V _c (m/min)	f (mm/rev)	t _c (min)	VB (mm)
2	80	0.05	10	0.070
3	80	0.05	15	0.086
4	80	0.1	5	0.077
6	80	0.1	15	0.164
7	80	0.15	5	0.067
8	80	0.15	10	0.111
10	115	0.05	5	0.071
11	115	0.05	10	0.091
12	115	0.05	15	0.111
15	115	0.1	15	0.151
16	115	0.15	5	0.077
17	115	0.15	10	0.112
20	150	0.05	10	0.098
21	150	0.05	15	0.148
22	150	0.1	5	0.083
24	150	0.1	15	0.144
25	150	0.15	5	0.081
26	150	0.15	10	0.120

Table 4 presents the testing dataset of 9 extra pairs, which were intentionally excluded from the training phase.

Table 4 – Testing dataset.

Test n°	Input variables			Measured flank wear
	V _c (m/min)	f (mm/rev)	t _c (min)	VB (mm)
1	80	0.05	5	0.047
5	80	0.1	10	0.111
9	80	0.15	15	0.143
13	115	0.1	5	0.076
14	115	0.1	10	0.104
18	115	0.15	15	0.133
19	150	0.05	5	0.074
23	150	0.1	10	0.106
27	150	0.15	15	0.158

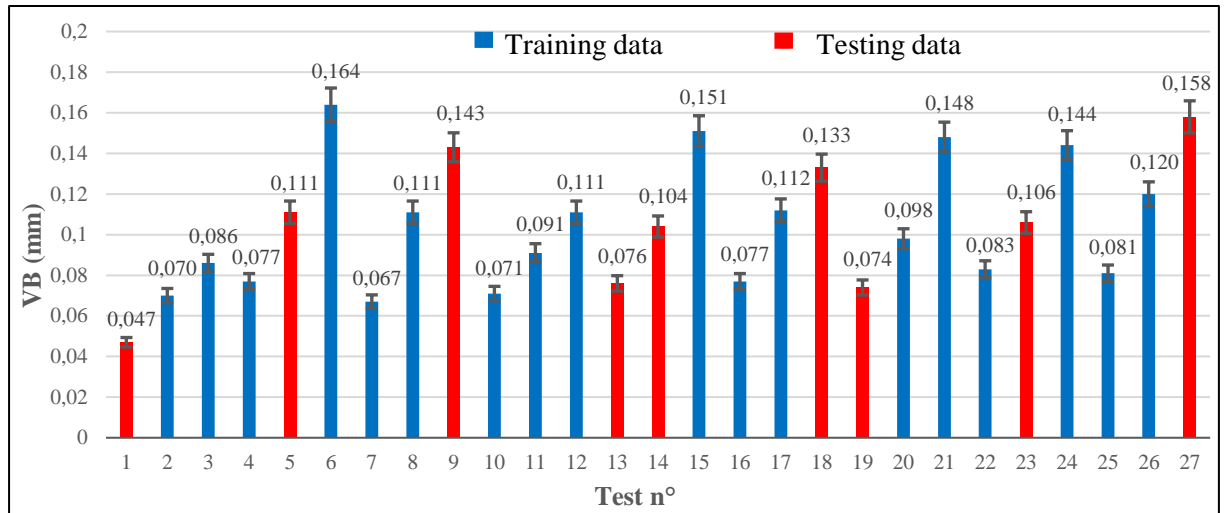


Figure 1 - Histogram of experimental data of (VB).

Figure 2 gives the flank wear (VB) plotted versus feed (f) and cutting time (t_c) for different values of cutting speed (V_c). For every combination of feed and cutting speed, the flank wear grows with cutting time. However, there is a complex relationship between these factors and tool wear. For this, we consider the present case of study six predictive models to determine the most powerful one.

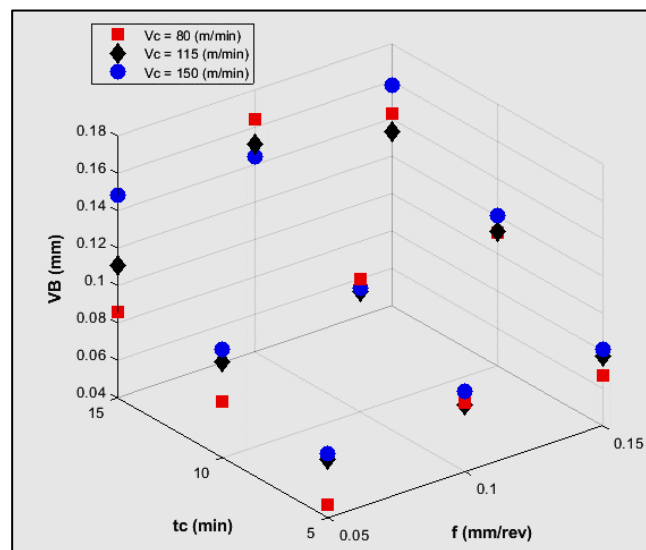


Figure 2 - Flank wear (VB) versus feed (f) and cutting time (t_c).

4. Simulation results

2.1. ANN Approach

The elaborated ANN using Matlab Neural Network Toolbox is depicted in the figure below. To ensure efficient processing, the vectors of inputs and observations are normalized within the range of (-1 to 1) before training and testing the network. The optimal design of the developed Artificial Neural Network employs a multilayer feed-forward structure with a 3-5-1 configuration, as depicted in Figure 3.

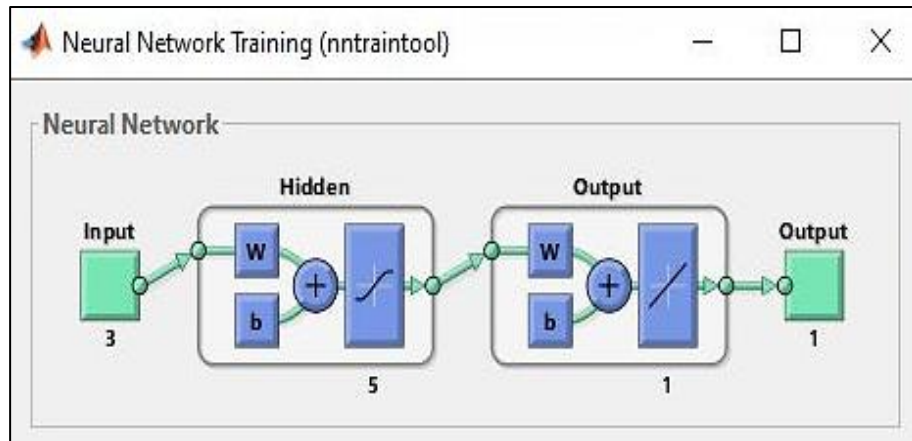


Figure 3 - Structure of the developed (ANN) using the Matlab.

Many simulations have indicated that opting for a single hidden layer yields give the most favorable results. Optimal outcomes were attained when employing a linear transfer function for the output layer, while a hyperbolic tangent sigmoid function was utilized for the hidden layer (Makhfi *et al.*, 2018; Mimoun *et al.*, 2022). Different training algorithms were tested; the stable state of the training process is obtained by using the Bayesian Regularization backpropagation.

In addition, through a series of simulations reported in Table 5, we selected the number of hidden neurons that yielded the highest linear regression coefficient (R) and minimal Mean Square Error (MSE) for the training phase. It is important to note that this was done to achieve optimal performance.

Table 5 – Choice of hidden neuron number.

Structure	R	MSE
3-2-1	0.9173	0.00014502
3-3-1	0.9175	0.00014476
3-4-1	0.9176	0.00014465
3-5-1	0.9176	0.00014458
3-6-1	0.9176	0.00014453
3-7-1	0.9176	0.00014450

From Table 5, we see that the ANN structure (3-5-1) is sufficient for training. We notice that the linear regression coefficient (R) stabilizes from several neurons equal to 5; however, MSE continues to decrease very slightly with the increase in the number of neurons.

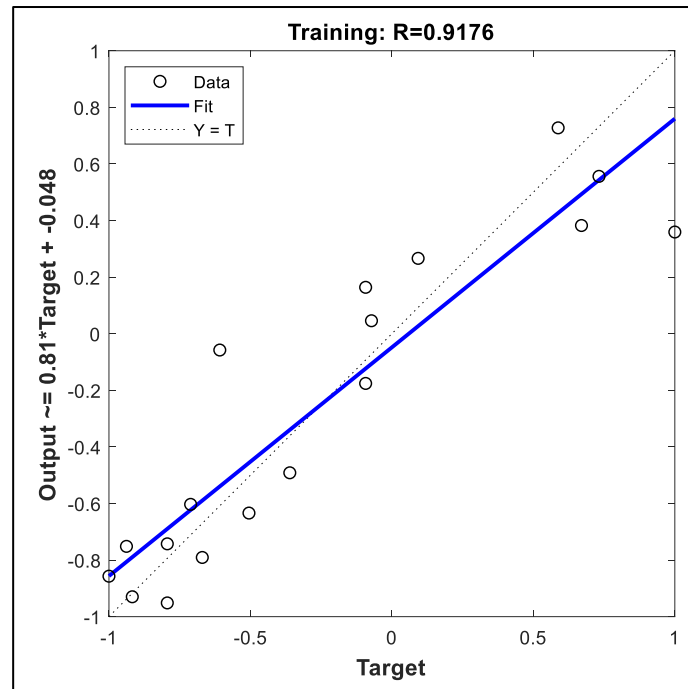


Figure 4 - Relationship between targets and predictive values of flank wear in the training phase.

Thus, to ensure rapid convergence and reduce simulation time, we can retain several neurons equal to 5. For the last, Fig. 4 shows the linear relationship between target and predictive values of flank wear in the training phase. In the training phase, the best performance is obtained at epoch 61 with $MSE = 0.00014458$ as shown in Figure 5.

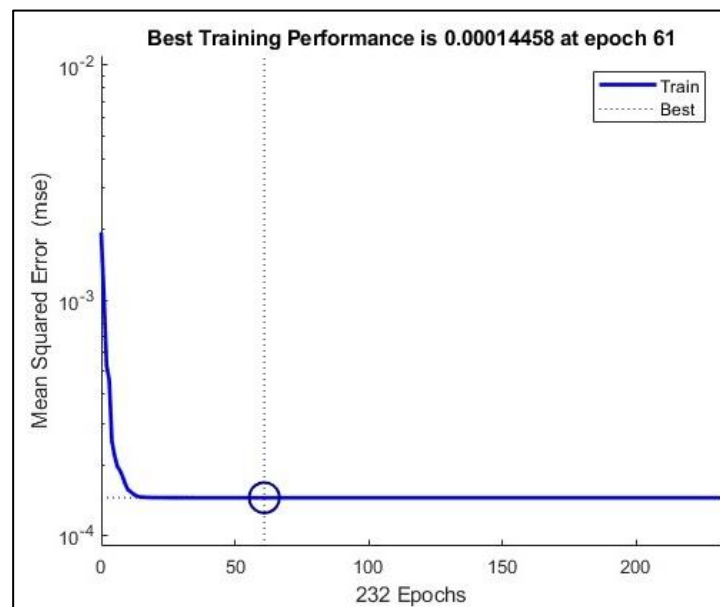


Figure 5 - Performance of the ANN at the training phase.

To train regression models including Gaussian Process Regression (GPR) and Support Vector Machine (SVM), we use the Regression Learner Toolbox under Matlab software.

4.2. GPR model

All GPRs of different regression learner algorithms were trained, including Rational Quadratic, Squared Exponential, Matern 5/2, and Exponential. Figure 6 shows the linear relationship between target and predictive values of flank wear in the training phase.

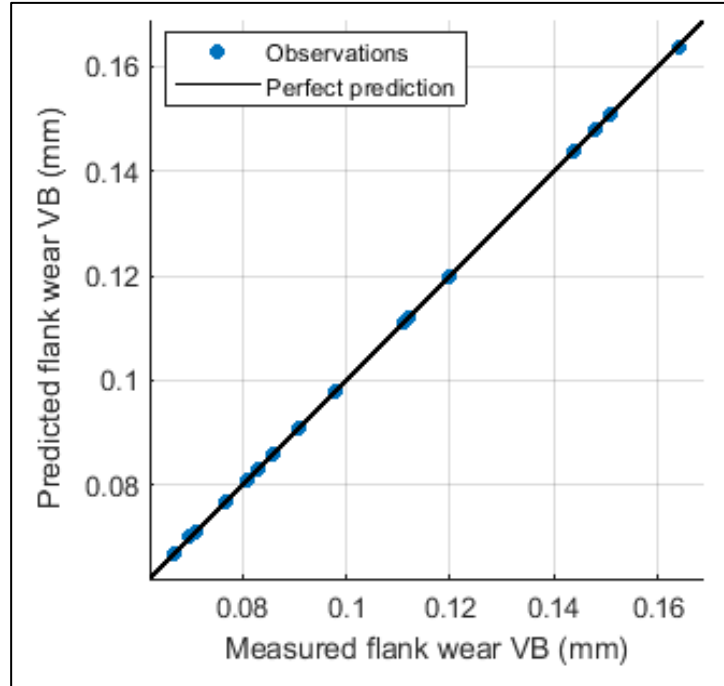


Figure 6 - Predicted vs measured flank wear for the GPR model.

4.3. SVM model

For the present study, the SVM model was trained by a Gaussian or Radial Basis Function (RBF) kernel given by Equation 6 (Gholami *et al.*, 2017; Kong *et al.*, 2017).

$$K(x_i, x_j) = G(x_i, x_j) = \exp\left(-\frac{\|x_i - x_j\|^2}{2\sigma^2}\right) \quad (6)$$

Where (σ^2) is the width parameter for optimization.

To fit the SVM model, six different kernel functions were investigated under Matlab software; they include linear, quadratic, cubic, fine Gaussian, medium Gaussian, and coarse Gaussian SVM. After all evaluations, the medium Gaussian is better than the other five SVMs, with automatic kernel scale and epsilon modes, and standardized data. Notice that for the Box Constraint, if we use automatic mode, the default value is calculated from the quartile deviation obtained from the box plot of the training data (see Table 6).

The default Box Constraint value for the Gaussian kernel function is $\text{iqr}(\text{VB})/1.349$, where $\text{iqr}(\text{VB})$ is the interquartile range of the response variable (VB). The $\text{iqr}(\text{VB})$ is the difference between the 3rd Quartile and the first Quartile. To obtain good performances in the training phase, the Box Constraint value is taken equal to one. Notice that under Matlab software, this value is set equal to one for all kernel functions except the Gaussian.

Table 6 – Values for Box plot of VB (Training data).

Statistic	VB
Number of observations	18
Minimum	0.067
Maximum	0.164
1 st Quartile	0.078
Median	0.095
3 rd Quartile	0.118
Mean	0.103
Variance (n-1)	0.001
Standard deviation (n-1)	0.031

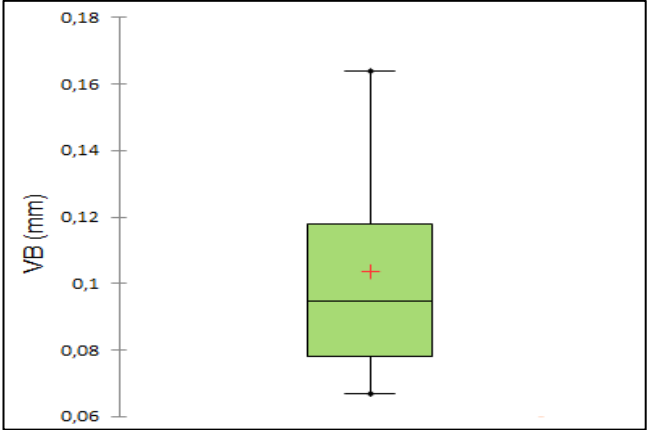
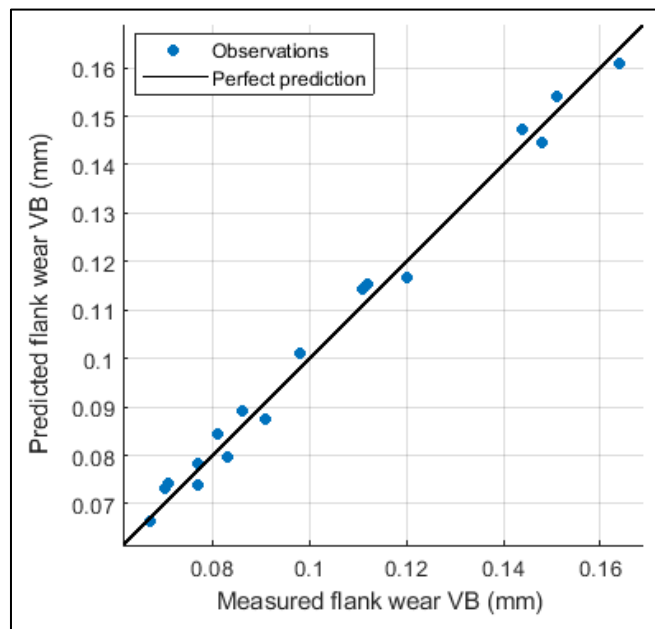


Figure 7 shows the linear relationship between target and predictive values of flank wear in the training phase. We conclude that the training is acceptably done with the SVM model.

**Figure 7 - Predicted vs measured flank wear for the SVM model.**

4.4. GAPOLYFITN model

We used the GAPOLYFITN function under Matlab software; by varying the number of terms and powers, the maximum number of generations is set to 50. The optimum structure is obtained from the results reported in Table 7.

Table 7 – Choice of the GAPOLYFITN structure.

Structure	R ²	MSE
3-1	0.987	0.000178
3-2	0.983	0.000222
3-3	0.991	0.000124
3-4	0.990	0.000133
3-5	0.985	0.000205

Note that the structure corresponds to the choice of the maximum number of terms and powers (maxterm-maxpower). From the last table, we see that the best structure is obtained for three terms and three powers because it gives the higher R^2 and minimal MSE. The fitted model is expressed by Equation 7:

$$VB = 0.00030511 \cdot V_c - 0.5515 \cdot f^2 \cdot t_c + 0.1328 \cdot f \cdot t_c \quad (7)$$

5. Performance indicators of the predictive models

To assess the statistical performance of the elaborated models, the following indicators were utilized: R^2 , MSE, and MAPE (Makhfi *et al.*, 2018; Mimoun *et al.*, 2022). These measures were employed to compare the predictions with the corresponding experimental values.

- The R-squared statistic can be calculated using Equation 8:

$$R^2 = 1 - \frac{SSR}{SST} = 1 - \frac{\sum_{k=1}^N (c(k) - s(k))^2}{\sum_{k=1}^N (c(k) - \bar{c})^2} \quad (8)$$

Where (c) represents the observed values of (VB), (s) denotes the corresponding predictive values of (VB), (\bar{c}) signifies the mean of the observed (VB) values, and (N) represents the total number of experimental values of (VB).

For the MLR without intercept and GAPOLYFITN models, the SST is given by Equation 9:

$$SST = \sum_{k=1}^N (c(k))^2 \quad (9)$$

- The MSE is expressed by Equation 10:

$$MSE = \frac{1}{N} \sum_{k=1}^N (c(k) - s(k))^2 \quad (10)$$

- The MAE formulation is done in Equation 11:

$$MAE = \frac{1}{N} \sum_{k=1}^N |c(k) - s(k)| \quad (11)$$

- The MAPE formulation is given by Equation 12:

$$MAPE(\%) = 100 \times \frac{1}{N} \sum_{k=1}^N \frac{|c(k) - s(k)|}{c(k)} \quad (12)$$

5.1. Comparison between ANN, GPR and SVM for the training phase

Table 8 presents a summary of the performance comparison for the training phase among the predictive models based on based on learning process. For the training phase, the good performances are relative to the GPR model.

The simulation results achieved for the training phase with the ANN, GPR, and SVM models have been documented in Table 9.

Table 8 – Performance comparison for the training phase.

	ANN	GPR	SVM
R-Squared	0.84	1.00	0.99
MSE	0.000145	2.0762e-09	9.4623e-06
MAE	0.009335	3.178e-05	0.002986
MAPE %	8.94	0.03	3.03

Table 9 – Simulation results for the training phase.

Test n°	Experimental data of VB (mm) (Özel <i>et al.</i> , 2007)	Predicted values of VB (mm)		
		ANN	GPR	SVM
2	0.07	0.079	0.070	0.073
3	0.086	0.113	0.086	0.089
4	0.077	0.069	0.077	0.078
6	0.164	0.133	0.164	0.161
7	0.067	0.074	0.067	0.066
8	0.111	0.107	0.111	0.114
10	0.071	0.070	0.071	0.074
11	0.091	0.085	0.091	0.088
12	0.111	0.123	0.111	0.114
15	0.151	0.142	0.151	0.154
16	0.077	0.079	0.077	0.074
17	0.112	0.118	0.112	0.115
20	0.098	0.092	0.098	0.101
21	0.148	0.134	0.148	0.145
22	0.083	0.077	0.083	0.080
24	0.144	0.151	0.144	0.147
25	0.081	0.086	0.081	0.084
26	0.120	0.128	0.120	0.117

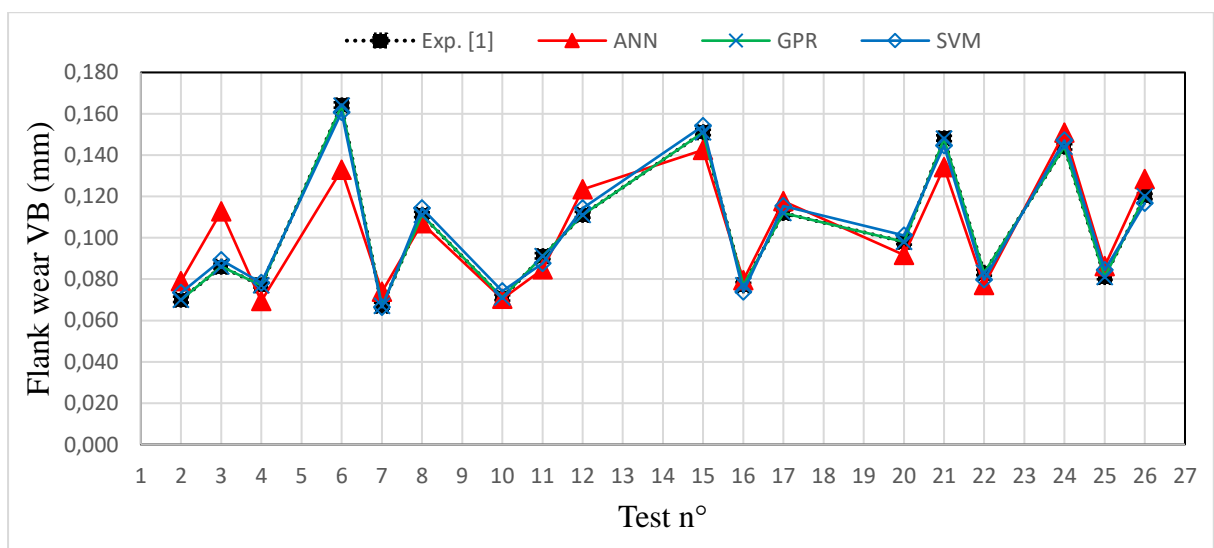
**Figure 8 - Confrontation between the experimental and predictive values (Training phase).**

Figure 8 shows a graphical confrontation during the training phase between experimental data and the values obtained from predictive models based on ANN, GPR, and SVM. Let us remember that from Figure 8, the predictive models based on GPR and SVM give the best performances in the training phase.

Table 10 presents a summary of the performance comparison for the testing phase among the predictive models based on learning process.

Table 10 – Performance comparison for the testing phase.

	ANN	GPR	SVM
R-Squared	0.86	0.90	0.74
MSE	0.00016178	0.00011882	0.00029611
MAE	0.009333	0.0088099	0.013816
MAPE %	10.95	10.44	14.51

For the testing phase, the good performances are relative to the GPR model. The simulation results achieved for the testing phase with the ANN, GPR, and SVM models have been documented in Table 11.

Table 11 – Simulation results for the testing phase.

Test n°	Experimental data of VB (mm) (Özel <i>et al.</i> , 2007)	Predicted values of VB (mm)		
		ANN	GPR	SVM
1	0.047	0.068	0.068	0.071
5	0.111	0.090	0.105	0.115
9	0.143	0.149	0.145	0.174
13	0.076	0.073	0.077	0.080
14	0.104	0.098	0.109	0.115
18	0.133	0.155	0.145	0.158
19	0.074	0.073	0.081	0.072
23	0.106	0.108	0.113	0.112
27	0.158	0.160	0.140	0.141

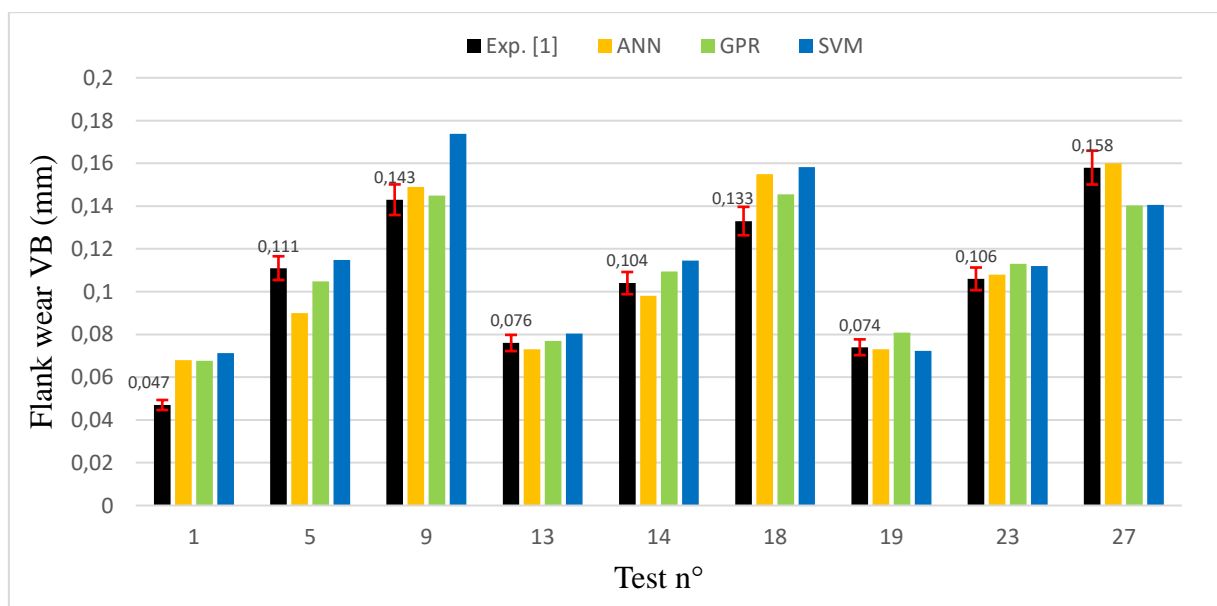


Figure 9 - Confrontation between the experimental and predictive values (Testing phase).

From Figure 9, we can see that the ANN approach performs better in the testing phase compared to the SVM which had better training performances. In addition, the GPR model gives the finest performances in the testing phase.

5.2. Performances comparison for the predictive models of flank wear

Table 12 presents a summary of the performance comparison among the six predictive models.

Table 12 – Performance comparison.

	ANN	GPR	SVM	GAPOLYFITN
R-Squared	0.85	0.96	0.89	0.99
MSE	0.000177	0.000046	0.000123	0.000124
MAE	0.009336	0.002958	0.006596	0.007816
MAPE %	9.60	3.50	6.86	7.54

Table 12 shows that the R-Squared statistic ranges from 0.85 to 0.99, the MSE is between 0.000046 and 0.000177, the MAE ranges from 0.002958 to 0.009336, and the value of MAPE varies from 3.50 to 9.60%. The predictive capability of GPR and GAPOLYFITN in determining flank wear is the best.

Figure 10 shows a graphical confrontation between experimental data and the values obtained from the predictive models (ANN, GPR, SVM and GAPOLTFITN).

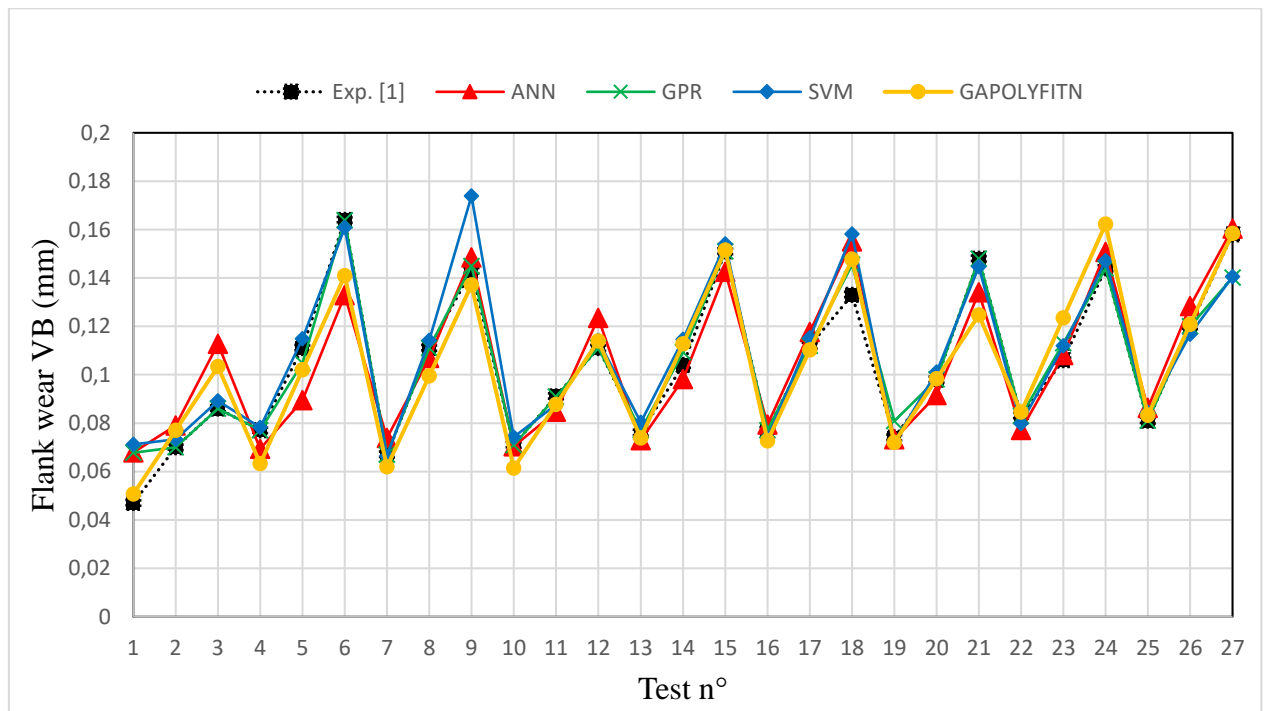


Figure 10 - Confrontation between the experimental and predictive values for the predictive models (ANN, GPR, SVM and GAPOLTFITN).

Table A-1 gives a numerical confrontation between experimental data and the values obtained from the predictive models (ANN, GPR, SVM and GAPOLTFITN). The powerful predictive model of flank wear is the GPR because it provides a good fit with the max. of the observations

6. Conclusions

This study aims to establish an efficient model for estimating flank wear in the hard turning of AISI D2 steel using a mixed alumina insert. To accomplish this, a comparative analysis was conducted, evaluating the performance of ANN, GPR, SVM and GAPOLTFITN models for predicting flank wear. The predictive models in this study utilized an experimental machining dataset comprising 27 samples. The inputs for these models are the factors: feed, cutting speed, and machining time.

- ✓ For the training phase, the good performances are relative to the GPR model with $R^2 = 1$, $MSE = 2.0762e-09$, and $MAPE = 0.03\%$.
- ✓ For the testing phase, the best performances are relative to the GPR model with $R^2 = 0.90$, $MSE = 0.00011882$ and $MAPE = 10.44\%$.
- ✓ We compared the flank wear predictions with experimental results to demonstrate the usefulness of the elaborated models. Through simulations conducted using Matlab software, the R-squared statistic ranges from 0.85 to 0.99, the MSE is between 0.000046 and 0.000177, the MAE ranges from 0.002958 to 0.009336, and the value of MAPE varies from 3.50 to 9.60%. The predictive capability of GAPOLYFITN and GPR in determining flank wear are the best, as they exhibit high (R^2), and lower values of MSE and MAPE. The powerful predictive model is the GPR because it provides $R^2 = 0.96$, $MSE = 4.6e-5$, $MAE = 0.002958$, and $MAPE = 3.50\%$.
- ✓ Models based on learning process hold great promise to predict the wear of cutting tools, however, the GAPOLYFITN model is more practical because it is a simple mathematical formulation that can be easily integrated, for example, into an adaptive control loop based on wear observation.

References

- Abdul, R. M., Minhat, M. B., Hussein, N., Salleh, M. (2018). A comprehensive review on cold work of AISI D2 tool steel. *Metall Res Technol*, 115, 104. <https://doi.org/10.1051/metal/2017048>
- Alajmi, M. S., Almeshal, A. M., (2021). Estimation and Optimization of Tool Wear in Conventional Turning of 709M40 Alloy Steel Using Support Vector Machine (SVM) with Bayesian Optimization. *Materials*, 14, 3773. <https://doi.org/10.3390/ma14143773>
- Arsecularatne, J. A., Zhang, L. C., Montross, C., Mathew, P. (2006). On machining of hardened AISI D2 steel with PCBN tools. *Journal of Materials Processing Technology*, 171, 244–252. <https://doi.org/10.1016/j.jmatprotec.2005.06.079>
- Bagga, P. J., Patel, K. M., Makhesana, M. A., et al (2023). Machine vision-based gradient-boosted tree and support vector regression for tool life prediction in turning. *Int J Adv Manuf Technol*, 126, 471–485. <https://doi.org/10.1007/s00170-023-11137-2>
- Bourithis, L., Papadimitriou, G. D., Sideris, J. (2006). Comparison of wear properties of tool steels AISI D2 and O1 with the same hardness. *Tribology International*, 39, 479–489. <https://doi.org/10.1016/j.triboint.2005.03.005>
- Choudhury, A., Sarma, D. K., Rajbongshi, S. K. (2023). Neural Network Modelling for Predicting Surface Finish and Flank Wear on AISI D2 Steel Machining. *Academic Journal of Manufacturing Engineering*, 21, 2. https://www.ajme.ro/PDF_AJME_2023_2/L6.pdf
- Clegg, J., Dawson, J. F., Porter, S. J., Barley, M. H. (2005). The Use of a Genetic Algorithm to Optimize the Functional Form of a Multi-dimensional Polynomial Fit to Experimental Data. In: 2005 IEEE Congress on Evolutionary Computation. IEEE, Edinburgh, Scotland, UK, 928–934. <https://doi.org/10.1109/CEC.2005.1554782>
- Davim, J. P., Figueira, L. (2007). Comparative evaluation of conventional and wiper ceramic tools on cutting forces, surface roughness, and tool wear in hard turning AISI D2 steel. Proceedings of the Institution of Mechanical Engineers, Part B: *Journal of Engineering Manufacture*, 221, 625–633. <https://doi.org/10.1243/09544054JEM762>

- Gholami, R., Fakhari, N. (2017). Support Vector Machine: Principles, Parameters, and Applications. In: Handbook of Neural Computation. Elsevier, 515–535. <https://doi.org/10.1016/B978-0-12-811318-9.00027-2>
- Hagan, M. T., Demuth, H. B., Beale, M. H., De Jesús, O. (2014). *Neural Network Design*. 2nd Edition eBook.
- Isabona, J., Imoize, A. L., Ojo, S., et al. (2023). Machine Learning-Based GPR with LBFGS Kernel Parameters Selection for Optimal Throughput Mining in 5G Wireless Networks. *Sustainability*, 15, 1678. <https://doi.org/10.3390/su15021678>
- Junaid, Mir. M., Wani, M. F. (2018). Modelling and analysis of tool wear and surface roughness in hard turning of AISI D2 steel using response surface methodology. *International Journal of Industrial Engineering Computations*, 63–74. <https://doi.org/10.5267/j.ijiec.2017.4.004>
- Khan, S. A., Ahmad, M. A., Saleem, M. Q., et al. (2017). High-feed turning of AISI D2 tool steel using multi-radii tool inserts: Tool life, material removed and workpiece surface integrity evaluation. *Materials and Manufacturing Processes*, 32, 670–677. <https://doi.org/10.1080/10426914.2016.1232815>
- Khan, S. A., Ameer, M. F., Uddin, G. M., et al. (2022). An in-depth analysis of tool wear mechanisms and surface integrity during high-speed hard turning of AISI D2 steel via novel inserts. *Int J Adv Manuf Technol*, 122, 4013–4028. <https://doi.org/10.1007/s00170-022-10151-0>
- Kong, D., Chen, Y., Li, N. (2018). Gaussian process regression for tool wear prediction. *Mechanical Systems and Signal Processing*, 104, 556–574. <https://doi.org/10.1016/j.ymsp.2017.11.021>
- Kong, D., Chen, Y., Li, N., Tan, S. (2017). Tool wear monitoring based on kernel principal component analysis and v-support vector regression. *Int J Adv Manuf Technol*, 89, 175–190. <https://doi.org/10.1007/s00170-016-9070-x>
- Makhfi, S., Haddouche, K., Bourdim, A., Habak, M. (2018). Modeling of machining force in hard turning process. *Mechanika*, 24, 3, 367–375. <http://dx.doi.org/10.5755/j01.mech.24.3.19146>
- Mimoun, C. H., Haddouche, K., Makhfi, S. (2022). A Comparative Study of Multiple Regression, ANN and Response Surface Method for Machining Force. Proc. of the Interdisciplinary Conference on Mechanics, Computers and Electrics (ICMECE 2022) 6-7 October 2022, Barcelona, Spain. <http://www.icmece.org/2022/proceedings.pdf>.
- Nazir, A. (2018). Influence of Wiper and Conventional Inserts at Profile Geometry During Turning of D2 Tool Steel. *ETOAJ*, 1. <https://doi.org/10.19080/ETOAJ.2018.01.555574>
- Nikolaus, I., Vollmer, Resul, A. I., Gürkan, Sin. (2021). Benchmarking of Surrogate Models for the Conceptual Process Design of Biorefineries, *Computer Aided Chemical Engineering*, Elsevier 50, 475–480. <https://doi.org/10.1016/B978-0-323-88506-5.50075-9>
- Özel, T., Karpat, Y., Figueira, L., Davim, J. P. (2007). Modelling of surface finish and tool flank wear in turning of AISI D2 steel with ceramic wiper inserts. *Journal of Materials Processing Technology*, 189, 192–198. <https://doi.org/10.1016/j.jmatprotec.2007.01.021>
- Quiza, R., Figueira, L., Davim, J. P. (2008). Comparing statistical models and artificial neural networks on predicting the tool wear in hard machining D2 AISI steel. *Int J Adv Manuf Technol*, 37, 641–648. <https://doi.org/10.1007/s00170-007-0999-7>
- Salcedo-Sanz, S., Rojo-Álvarez, J. L., Martínez-Ramón, M., Camps-Valls, G. (2014). Support vector machines in engineering: an overview. *WIREs Data Min & Knowledge Discovery*, 4, 234–267. <https://doi.org/10.1002/widm.1125>
- Schulz, E., Speekenbrink, M., Krause, A. A. (2018). Tutorial on Gaussian process regression: Modelling, exploring, and exploiting functions. *Journal of Mathematical Psychology*, 1–16. <https://doi.org/10.1101/095190>
- Tang, L., Sun, Y., Li, B., et al. (2019). Wear performance and mechanisms of PCBN tool in dry hard turning of AISI D2 hardened steel. *Tribology International*, 132, 228–236. <https://doi.org/10.1016/j.triboint.2018.12.026>

Yu, Liang., Shanshan, Hu., Wensen, Guo., Hongqun, Tang. (2022). Abrasive tool wear prediction based on an improved hybrid difference grey wolf algorithm for optimizing SVM, *Measurement*, 187, 110247. <https://doi.org/10.1016/j.measurement.2021.110247>

Appendix

The simulation results achieved with the six developed models have been documented in Table A-1.

Table A-1: Simulation results for the elaborated models.

Test n°	Experimental data of VB (mm) (Özel <i>et al.</i> , 2007)	Predicted values of VB (mm)			
		ANN	GPR	SVM	GAPOLYFITN
1	0.047	0.068	0,068	0.071	0.051
2	0.07	0.079	0,070	0.073	0.077
3	0.086	0.113	0,086	0.089	0.103
4	0.077	0.069	0,077	0.078	0.063
5	0.111	0.090	0,105	0.115	0.102
6	0.164	0.133	0,164	0.161	0.141
7	0.067	0.074	0,067	0.066	0.062
8	0.111	0.107	0,111	0.114	0.100
9	0.143	0.149	0,145	0.174	0.137
10	0.071	0.070	0,071	0.074	0.061
11	0.091	0.085	0,091	0.088	0.088
12	0.111	0.123	0,111	0.114	0.114
13	0.076	0.073	0,077	0.080	0.074
14	0.104	0.098	0,109	0.115	0.113
15	0.151	0.142	0,151	0.154	0.152
16	0.077	0.079	0,077	0.074	0.073
17	0.112	0.118	0,112	0.115	0.110
18	0.133	0.155	0,145	0.158	0.148
19	0.074	0.073	0,081	0.072	0.072
20	0.098	0.092	0,098	0.101	0.098
21	0.148	0.134	0,148	0.145	0.125
22	0.083	0.077	0,083	0.080	0.085
23	0.106	0.108	0,113	0.112	0.123
24	0.144	0.151	0,144	0.147	0.162
25	0.081	0.086	0,081	0.084	0.083
26	0.12	0.128	0,120	0.117	0.121
27	0.158	0.160	0,140	0.141	0.158